Supplemental Material: Robust capacity expansion planning in hydro-dominated power systems: A Nordic case study

Daniel M. Cox[a], Davi Rodrigues Damasceno[a], Johan Hagsten[a], Carl Hellesen[a], Martin Hjelmeland[b], Jakub Jurasz[a,e], Alexander Kies[f], Oscar Lagnelöv[a], Martin Lundberg[c], Lukas Lundström[a], Joseph T. K. McKenna[a], Per Norberg[a], Jonas Kristiansen Nøland[c], Albert Payaró Llisterri[a], Staffan Qvist[a], Sebastian Svanström[a], Anton Såmark-Roth[a,*,1], Ying Yang[a], Mohammad Reza Hesamzadeh[d] and Lina Bertling Tjernberg[d]

[a]*Quantified Carbon, United Kingdom, Sweden, Poland, Finland, Belgium, Spain & the Netherlands*

[b]*Department of Electric Energy, Norwegian University of Science and Technology (NTNU), O. S. Bragstads plass 2E, Trondheim, 7049, Norway*

[c]*Division of Industrial Electrical Engineering and Automation, Lund University, Lund, 221 00, Sweden*

[d]*School of Electrical Engineering and Computer Science, KTH Royal Institute of Technology, Stockholm, Sweden*

[e]*Department of Water Supply and Sewerage Systems, Wrocław University of Science and Technology, Wrocław, 50-384, Poland*

[f]*Department of Electrical and Computer Engineering, Aarhus University, Aarhus, 8200, Denmark*

ARTICLE INFO

ABSTRACT

This supplemental material provides comprehensive insights into the assumptions, tools, and methodologies that support the capacity expansion analysis in the main study. Central to the modeling process is the *Weather2Energy* tool, which generates wind and solar production profiles from historical and projected weather data to simulate renewable energy outputs. In addition, the tool produces heating and cooling demand profiles, offering a complete view of how energy demand fluctuates in response to seasonal and daily weather variations. The supplemental material also includes a detailed report on the key assumptions underlying the case study, which focuses on the year 2050. This case study is designed to establish the most sustainable and competitive power system configuration, whilst ensuring security of supply, for Sweden's future energy landscape. Three sensitivities—reference, optimistic, and conservative—are explored to assess the impacts of varying key parameters on the Swedish power system across a wide range of scenarios. It is important to note that the main paper merely focuses on the reference sensitivity. The assumptions covered in this document include detailed investment and operational costs, technical parameters, maximum expansion limits for onshore and offshore wind, geographical modeling regions, transmission infrastructure, demand profiles, and associated flexibility. Additionally, it outlines exogenous factors such as existing capacities, offering a solid foundation for capacity expansion analyses presented in the main study and potentially elsewhere.

1. Weather2Energy

Weather2Energy is a set of tools that produce wind and solar production profiles as well as heating and cooling demand profiles.

1.1. Wind and solar production profiles

The calculation method for wind power capacity factor times series is summarized in Figure 1. It involves the five main steps described below:

1. Datasets of existing and planned wind park localisation. The Wind Power [1] dataset is used as basis. For Sweden, national permitting data is used [2].

2. ERA5 is a state-of-the-art climate dataset produced by the European Centre for Medium-Range Weather Forecasts as part of the Copernicus Climate Change Service. ERA5 includes a wide range of meteorological parameters, such as temperature, precipitation, solar radiation, and wind speed, at a high spatial resolution of 0.25 degrees (about 31 km horizontal resolution). According to analysis by Ref. [3]

ERA5 performs as good or somewhat better than MERRA-2 (another often used re-analysis dataset) for wind power analysis. The wind components at 100-meter height are used as basis for the wind power calculations.

3. The global ERA5 reanalysis climate data has a horizontal resolution of 31 km and does not account for mesoscale or microscale topography. To increase the resolution, it is downscaled using data from Global Wind Atlas (GWA) version 3.3. GWA is a comprehensive and authoritative online resource developed by DTU Wind Energy for the renewable energy sector and academic research that accounts for topographical information at the microscale. It uses ERA5 wind data for the years 2008-2017 as input, thus the available downscaled products are an average of that period.

The mean adjust factor (3b in Fig. 1) uses the GWA 3.3 average wind speed product at 100-meter height and resolution of 0.25 km as input. This matrix is in a first step coarsened to a resolution of 2.5 km. Next this matrix is divided by the ERA5 2008-2017 average wind speed at 100 m and at the original approximately 31 km horizontal resolution, thus resulting in a forcing factor matrix of 2.5 km resolution.

---

*Corresponding author

✉ anton@quantifiedcarbon.com (Anton Såmark-Roth)
ORCID(s): 0000-0003-3284-5748 (Anton Såmark-Roth)

The shear exponent (3c in Fig. 1) uses the GWA 3.3. average wind speed products at 100-meter and at 150-meter height at resolution of 0.25 km as input. These matrices are in a first step coarsened to a resolution of 2.5 km and the shear exponent between 100 to 150 meter height is calculated as:

$$\alpha = \ln\left(\frac{U^{gwa}_{100m}}{U^{gwa}_{150m}}\right) / \ln\left(\frac{100m}{150m}\right), \quad (1)$$

where U^{gwa}_{100m} and U^{gwa}_{150m} are the GWA average wind speeds at 100 and 150 meters, respectively.

4. In this step hourly wind output per wind park is calculated. The hourly wind speed at hub height (U_{hh}) of the park is calculated as follows:

$$U_{hh} = U^{era5}_{100m} \cdot f \cdot (hh/100m)^{\alpha}, \quad (2)$$

where U^{era5}_{100m} is the hourly wind speed at 100 meter height from the closest ERA5 grid, f is the ERA5 to GWA mean bias adjustment factor, and $(hh/100m)^{\alpha}$ does the vertical extrapolation from 100 m to wanted hub height (hh).

The wind power output is calculated as a function of the power curve of the turbine make and model. Actual power curves from the Ref. [1] are used for existing parks where turbine make information is available (visualised in 4b in Figure 1), but smoothed using the heuristic smoothing function defined in eq. 4 of Ref. [4] as to better represent wind power generation of wind parks.

The turbine availability is modelled as a simple function of time, where new turbines are assumed to have an availability of 95% while turbines older than 15 years are given a linearly diminishing availability (visualised in 4c in Figure 1), both to reflect larger fail ratios of older turbines and that the datasets might mislabel some older parks as operational though they are decommissioned.

5. The final step aggregates the hourly wind generation within bidding zones and then divides with installed capacity to get hourly capacity factors.

1.2. Demand profiles

Underlying methodology determining the profiles of the demand categories included in the modelling is presented here. Excerpts of the demand profiles and their associated flexibility is covered in Sec. 2.5 and in Fig. 7. A baseline hourly profile, aiming to represent weather-independent demand, primarily comprising the residential & tertiary demand category, is created for each bidding zone z as follows:

$$d^{bl}_{t,y,z} = d^{ERAA}_{t,y,z} - d^{s}_{t,y,z} - d^{EV}_{t,y,z} - d^{H}_{t,y,z} - d^{C}_{t,y,z} \text{ [MWh], (3)}$$

where the subscripts t, y, z denotes the time t, the model year y and the bidding zone z. d^{ERAA} is an hourly total demand profile from ENTSO-E European Resource Adequacy Assessment (ERAA)[1] (detailed methodology in Ref. [5]) representing model year y 2024. d^{s} is an hourly profile for
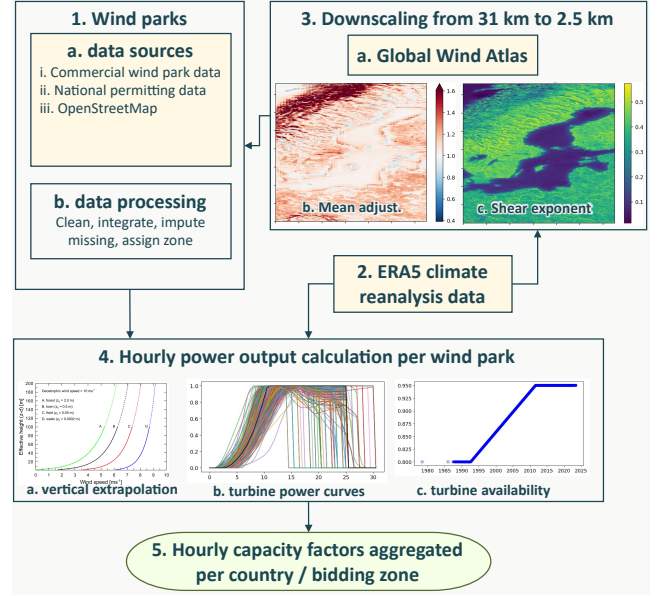
Figure 1: Schematic overview of the wind profile creation.

heating sanitary water, d^{EV} is a profile for charging electric vehicles (EV), d^{H} and d^{C} are the profiles for space heating and space cooling respectively.

Profiles for sanitary hot water and EV's (the type A profile, with a diurnal and weekday pattern typical of private cars) are taken from Ref. [5]).

Hourly space heating and space cooling are modelled as follows:

$$d^{H}_{t,y,z} = \beta^{H}_{z,y} I^{H}_{t,z} \quad \text{and} \quad d^{C}_{t,y,z} = \beta^{C}_{z,y} I^{C}_{t,z}, \quad (4)$$

where I^{H} and I^{C} are hourly heating and cooling indexes (see equations 5 and 6), and β^{H} and β^{C} are coefficients that describe the need for heating and cooling per centigrade [MW/°C]. The β coefficients representing year 2024 are identified for each zone using regression analysis with the heating and cooling indices and the d^{ERAA} total load. Figure 2 shows results from the regression analysis using both actual total load data and the d^{ERAA} total load, the coefficients are further divided by the population count to allow between zonal comparison in watt per centigrade [W/°C] per capita.

1.2.1. Heating and cooling indexes

A heating index (I^{H}) is calculated as follow

$$I^{H} = \begin{cases} 0 & \text{if } T^{eq} > T^{b}, \\ T^{b} - 0.5(T^{eq} + T^{p05}), & \text{if } T^{eq} < T^{p05}, \\ T^{b} - T^{eq} & \text{otherwise} \end{cases} \quad (5)$$

where T^{eq} are temperature equivalents (see Ref. [6] for detailed calculation procedure) where ambient temperature is the most important variable but also effects from solar, wind, and thermal inertia is accounted for to get one single linearized variable describing the impact of weather on
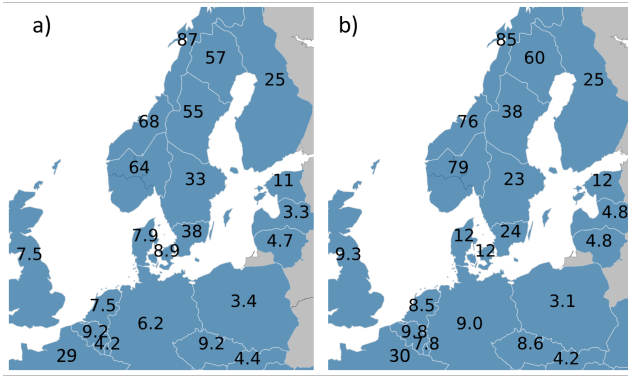
Figure 2: Watt per centigrade and capita, (a) estimated from actual total load data from the winter 2020/21 (b) estimated from the ERAA load data of model year 2024.

heat and cooling demand. The parameter T^b is the base temperature under which heating need starts (16°C is used), T^{p05} is the 5% percentile of the T^{eq} (determined from the 1990-2019 period) under which the heating demand increase is assumed to slow down as heating systems approach their designed maximum capacities.

A similar approach is used to calculate a cooling index (I^C), but using the 95th percentile and a base temperature (T^b) of 25°C, as shown in eq. 6 below:

$$I^C = \begin{cases} 0 & \text{if } T^{eq} < T^b, \\ 0.5(T^{eq} + T^{p95}) - T^b, & \text{if } T^{eq} > T^{p95}, \\ T^{eq} - T^b & \text{otherwise} \end{cases} \quad (6)$$

To obtain a heating and a cooling index representative of a whole region, such as an electricity bidding zone, gridded reanalysis weather data ERA5 [7] is weighted with gridded population count data [8] as proxy for the location of heat and cooling demand.

2. Case study

The case study is designed to establish the most sustainable and competitive power system configuration, ensuring security of supply, for a decarbonised Swedish economy in 2050. While the main paper describes the employed methodology, the following sections compiles the key assumptions underlying the case study.

2.1. CO2 Emissions

In this study, a CO2 price of 263 €/tCO2 is assumed as the primary driver for decarbonisation and emission reduction. This value aligns closely with the projection in Ref. [9], which estimates a CO2 price of 250 €/tCO2 by 2050 for advanced economies committed to net-zero emissions. Additionally, it is assumed that all existing fossil-fuelled power plants within the Swedish power system are retired. The only remaining technology with direct CO2 emissions allowed in the capacity expansion is the natural-gas-fuelled

Table 1
Upper expansion limits in GW for onshore and offshore wind for the indicated sensitivities employed in the modelling.

	Sensitivity	SE1	SE2	SE3	SE4
	Optimistic	13.3	18.7	14.5	4.6
Wind Onshore	Reference	8.2	11.4	10.3	3.6
	Conservative	5.4	7.6	6.9	2.4
Wind Offshore	Reference	5.1	-	-	-

open-cycle gas turbine power plants (denoted Gas OC), along with power plants running on bio-based fuels.

2.2. Onshore and offshore wind expansion limits

The Nordic countries, especially northern Sweden and Finland, are characterized by weather conditions highly favourable to onshore wind energy generation [10]. However, significant portions of the land area in northern Sweden, encompassing most of bidding zones SE1 and SE2, face pronounced conflicts of interest. This arises because the region is historically inhabited by the Sami indigenous people, and much of it comprises pristine natural landscapes protected as world heritage sites, nature reserves, national parks, valuable state-owned forests, and wetlands (among other overlapping protected categories), alongside significant military interest areas.

In contrast, southern Sweden's bidding zones, SE3 and SE4, exhibit considerably higher population densities. Consequently, challenges related to land availability, public acceptance, and permitting processes pose significant constraints on the potential expansion of onshore wind energy projects [11].

The current study employs the bidding-zone specific maximum expansion limits as presented in Table 1. The sensitivities have been based on the long-term market analysis (LMA) published in 2024 by the Swedish TSO, Svenska Kraftnät (SvK), and the scenarios Elektrifiering Förnybart (EF) and Elektrifiering Planerbart (EP) for the year 2045 [12]. The conservative sensitivity (SvK LMA 2024 (EP)·0.8) represents a scenario where only mature projects in the current pipeline materialize, e.g., due to issues with local opposition. In contrast, the optimistic sensitivity (SvK LMA 2024 (EF)·1.1) assumes the realization of all projects in the pipeline and planned phases, with additional projects becoming feasible as more land becomes available for onshore wind. Finally, the reference sensitivity (SvK LMA 2024 (EP)·1.2) represents a scenario where all projects in the pipeline as well as most projects in the planning phase materialize. Figure 3 presents the total maximum yearly generation for the optimistic, reference and conservative sensitivities and compares it to Ref. [12].

Correspondingly, the expansion limit for offshore wind at 5100 MW in bidding zone SE1 was set based on the maximum expansion observed in Ref. [12], further given in Table 1. In the vicinity of the remaining bidding zones SE2, SE3 and SE4, there is a very large potential for the expansion of offshore wind power relative to the demand growth [11].
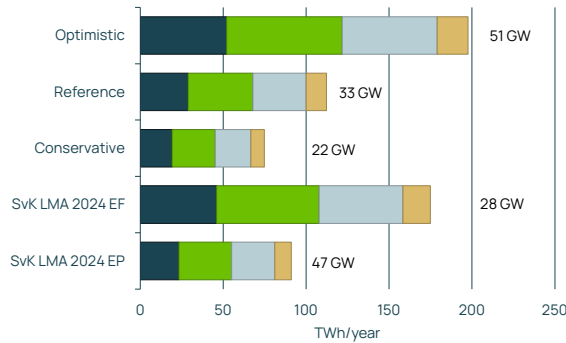
Figure 3: Total estimated maximum yearly generation for onshore wind, derived from the installed capacity and an average capacity factor 0.38, for the sensitivities employed in the current work (top three rows) compared to scenarios in Ref. [12]. Installed capacity in entire Sweden is indicated with the text following each bar.

On this background, no upper limit on the offshore wind expansion was defined for SE2, SE3 and SE4.

Notably, the present-day installed capacity of onshore wind sums up to 19.5 GW for all of Sweden [13]. With an assumed technical lifetime of 30 years only a small amount of this capacity is likely present in 2050. On this background, the model builds onshore wind from scratch.

2.3. Modelling regions and transmission

When setting up the geographical scope of the model, a balance must be struck between achieving sufficient accuracy and managing computational complexity. To reduce calculation time without introducing simplifications that could distort electricity market modelling, an analysis was conducted to determine which bidding zones could be merged or excluded. The analysis suggested merging southern Norway's bidding zones (NO1, NO2, NO5, collectively denoted *NO125*) and the Baltic states (Estonia, Latvia, and Lithuania, denoted *BT*), as this would significantly reduce computational time while having minimal impact on market dynamics. As a result, the geographical scope of the study has been limited to the zones shown in Fig. 4[2].

The maximum transmission capacities for the 29 lines included in the model are included in Fig. 4. These assumptions are primarily based on the investment plans of national TSOs, which have been compiled in sources such as Ref. [14]. Notably, the GenX simulations do not include bidding zones UK, NL, FR and ES[3].

For this study, we have adopted a transmission expansion cost assumption of 1.5 M€$_{2023}$/km. This choice is informed by budgeted costs for transmission expansion in Sweden [15], as well as contemporary cost evaluations derived from Norwegian transmission line projects [16], as detailed in Table 2. While the chosen value of 1.5 M€/km is nominally above inflation-adjusted figures in Table 2, it's important to

---

[2]Spain (ES) is also included but not shown in Fig 4.
[3]Not included in figure. Assumed transmission capacity FR-ES of 2600 MW.
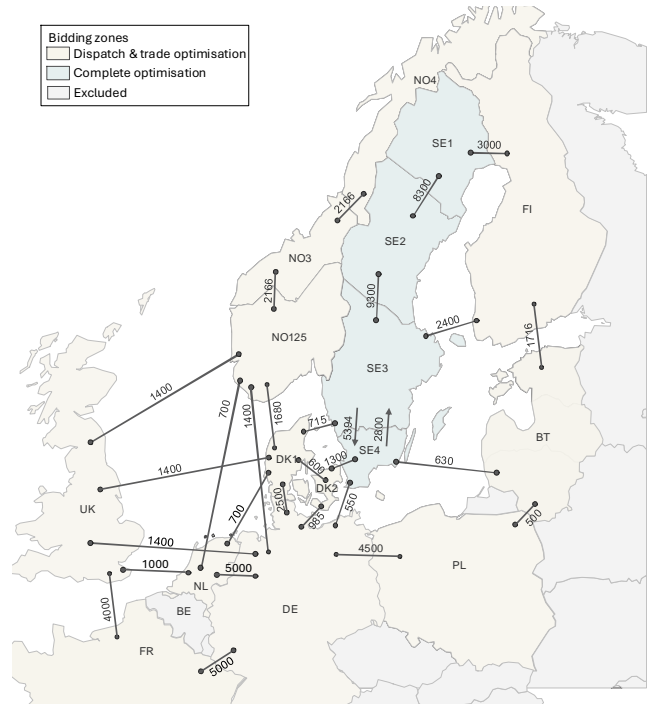

Figure 4: Geographical boundaries with regions included in the modelling and how they are treated in the optimisation. Lines represent transmission part of the modelling and the numbers and line sizes represent the associated net transfer capacity (MW) for model year 2050. The zones *NO125* and *BT* represents an aggregate of NO1, NO2 and NO5 the Baltic zones, respectively.

Table 2

Cost of recent transmission line construction projects in Norway [16]. Exchange rate is set to 10 NOK/€ and values are inflation adjusted from 2019 to 2023.

	Total cost [M€$_{2023}$/km]	Distance [km]	Construction year
Bamble-Rød	1.30	38	2013-2015
Namsos-Hofstad	0.95	82	2016-2018
Ofoten-Balsfjord	1.20	153	2014-2017
Sima-Samnanger	1.28	92	2010-2013

consider that this adjustment reflects changes in the consumer price index. Moreover, it is reasonable to assume that large-scale transmission expansion include transformer station upgrades, which introduce additional costs not reflected in Table 2.

The model can expand the transmission capacities for the lines within Sweden. Associated direct and annual investment costs are presented in Table 3, with an assumed lifetime of 60 years for overhead lines (OHL) and 40 years for High-Voltage Direct Current lines (HVDC) and a weighted average cost of capital of 6%. The time from decision to operation is for OHL > 10 years, for HVDC cable projects it could be < 5 years [17]. Costs have been calculated from the average lengths of the existing lines between the areas.

Table 3
Overnight and annual investment costs for the transmission lines allowed to expand capacities between bidding zones for the 2050 model year.

Transmission line	Overnight costs [k€/MW]	Annual investment costs [k€/MW]
SE1-SE2	720	45
SE2-SE3	580	36
SE3-SE4	290	18

Figure 5: Annual power demand presented by scenario and demand category.

The internal cost for connecting production or consumption to the existing main grid is not included.

Notably, the assumed transmission capacity in the reference scenario between SE1 and SE2 is assumed to increase substantially by 2050 from its current 3300 MW to 8300 MW (see Fig. 4). The reason is that in the model, most of the hydrogen production for industrial use in SE1 could also be produced in SE2. This would result in a severe bottleneck between SE1 and SE2 with wind power production being locked into SE2. A realistic scenario would be to produce parts of the hydrogen locally in SE2 and transport it to SE1 in a pipeline, which typically has an equivalent capacity of about 5 GW. Since hydrogen trade is currently neither a part of GenX nor cGrid, an equivalent electric transmission is added instead.

Additional assumptions regarding transmission capacities are as follows:

- Reinvestments to keep the existing Swedish national grid running (220 kV and 400 kV) with current transmission capacity between the Swedish bidding zones and international connections are assumed to take place in all modelling cases. The costs for this have therefore been excluded from the optimisation calculations.

- Reinvestments and new investments to maintain and expand the existing Swedish subtransmission and distribution networks are assumed to take place in all modelling cases. These have therefore been excluded from the optimisation calculations. In total, investments of at least 50 billion € in Sweden at all network levels during the period 2022–2050 are included in all modelled scenarios.

- Infrastructure investments related to the production, transmission, and storage of hydrogen have been excluded in the optimisation. These investments are however expected to be significant. To reflect the development of a hydrogen pipeline transmission network, the power transmission capacity between SE1 and SE2 has been increased with 5 GW. The investments are primarily to be carried by consumers (as such costs should not be added to the system), however they provide the power system valuable flexibility.
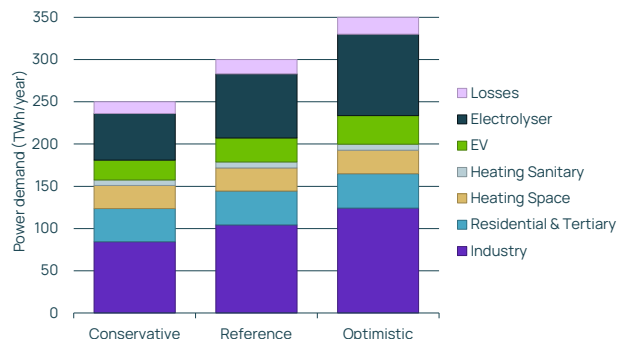
2.4. Demand scenarios

Demand scenarios have been developed based on the most recent long-term analysis conducted by the Swedish TSO in Ref. [12]. The optimistic and conservative scenarios are derived from the *Elektrifiering Förnybart* and *Elektrifiering Planerbart* scenarios, respectively. The reference scenario is determined as the average of these optimistic and conservative projections. To ensure alignment with recent Swedish energy policy targets [18], the final yearly demand has been scaled such that the reference scenario totals 300 TWh, the optimistic scenario corresponding to 350 TWh and the conservative scenario to 250 TWh.

Figure 5 illustrates the resulting demand for the model year 2050, broken down by demand category across the different scenarios. The categorisation of demand has been informed by four key aspects: (i) availability of data, (ii) demand and growth potential and associated uncertainty, (iii) divergent demand profiles and (iv) flexibility behavior and potential.
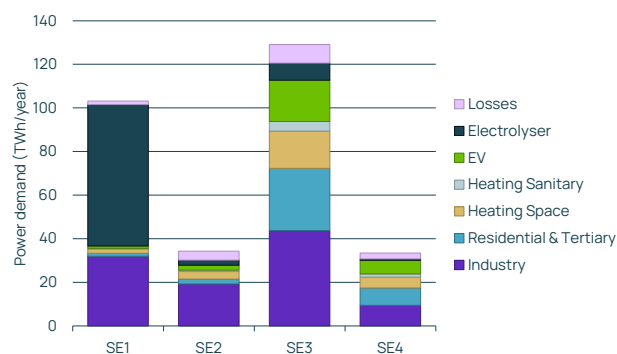

Figure 6: Annual power demand presented by Swedish bidding zone and demand category for the reference demand scenario.

The demand by bidding zone for the reference scenario totalling 300 TWh for Sweden is shown in Fig. 6. In synergy with the reinforced transmission capacity between SE1 and SE2 representing hydrogen pipelines introduced in Sec. 2.3, electrolyser demand is split between SE1 and SE2 in the reference scenario. Consistently, 28% of the electrolyser demand in SE1 is moved to SE2 which corresponds to 18 TWh
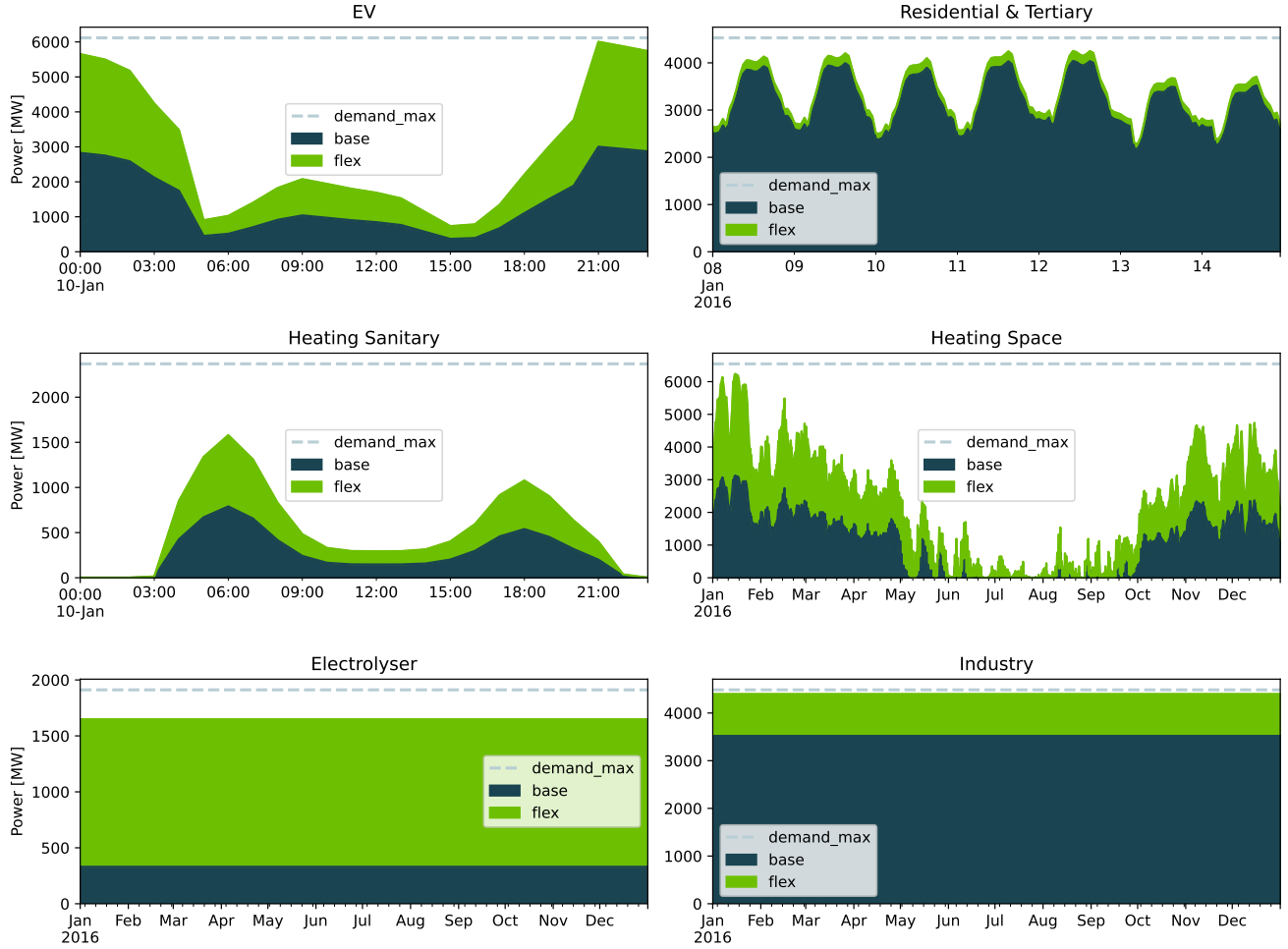
Figure 7: Demand profiles for the SE3 bidding zone in 2050, categorized by flexibility type as indicated in each panel. The *base* and *flex* areas represent demand segments where cutting and shifting flexibility are applied, respectively. The dashed line indicates the maximum capacity increase allowed for demand. The x-axis illustrates different time scales and windows, highlighting key periods of interest for the weather year 2016.

in the reference demand scenario which totals 300 TWh for Sweden.

2.5. Demand-side flexibility

The current case study employs the assumptions carefully described in Appendix C of Ref. [19]. The notations used here are derived from the main paper. For more detailed modelling methodology, the reader is referred to the main text.

The demand is split into the following six different flexible categories: electrolyser, water heating, space heating, residential & tertiary, industry and electric vehicles. The demand time series for a given category d_t^c is calculated as a category-specific normalised profile ($d_t^{\text{prof},c}$) times the overall demand ($d^{\text{total},c}$) in this category:

$$d_t^c = d_t^{\text{prof},c} \cdot d^{\text{total},c}. \tag{7}$$

The model incorporates two types of demand side flexibility: shifting and cutting. For shifting, three parameters are relevant. First, the $f_{\text{share}}^{\text{flex},c}$ describes the share of the

category-specific demand that is flexible and can be shifted in time. The demand for which shifting flexibility is applied is calculated via:

$$d_t^{\text{flex},c} = f_{\text{share}}^{\text{flex},c} \cdot d_t^c. \tag{8}$$

The second parameter $f_{\text{max}}^{\text{flex},c}$ describes the fraction of the maximum capacity of the demand profile until which the demand can be increased[4]. The third parameter, τ, describes a maximum time duration within which the flexible load can be shifted both forward and backward. By definition, a value for τ of n hours means, that the load at a specific time step can be shifted in either direction by $\frac{n}{2}$ hours.

The second type of demand flexibility included in the modelling approach is demand cutting. The base share of the demand, $d_t^{\text{base},c}$,

$$d_t^{\text{base},c} = \left(1 - f_{\text{share}}^{\text{flex},c}\right) \cdot d_t^c, \tag{9}$$

---

[4]A corresponding minimum fraction, $f_{\text{min}}^{\text{flex},c}$, has been set to 0 for all categories.

Table 4
Parameters for demand flexibility. The column f_{max}^{flex} the fraction of the maximum capacity of the demand profile until which the demand can be increased, given as a fraction. τ is given in hours, $1 - \sigma_2$, representing the share of the base demand for which cutting flexibility is applied, is given in % and p_{low}, p_{high} are given in €/MWh. Assumptions for the electrolyser category is provided for the optimistic (Opt.), reference (Ref.) and the conservative (Con.) sensitivities.

Category	f_{max}^{flex}	τ [h]	$1 - \sigma_2$ [%]	$[p_{low}, p_{high}]$
Electric Vehicles	1.0	24	0	-
Space Heating	1.1	4	5	100,1000
Sanitary Heating	2	12	5	100,1000
Industry	1	4	30	100,1000
Residential & Tert.	1	4	5	100,1000
Electrolyser Opt.	1.4	10	0	-
Electrolyser Ref.	1.2	10	5	80,200
Electrolyser Con.	1.1	10	20	80,200

Table 5
Flexible share $(f_{share}^{flex,c})$ for the demand categories in 2050 for the three different sensitivities. Shares are given in %.

Category	Optimistic	Reference	Conservative
Electric Vehicles	80	50	20
Space Heating	90	50	10
Sanitary Heating	90	50	10
Industry	40	20	0
Resid. & Tert.	20	5	0
Electrolyser	100	80	60

can be cut. This process represents consumers cutting their demand when electricity prices are too high. The base demand is linearly cut within the electricity price interval $[p_{low}, p_{high}]$ until the minimum demand fraction, denoted σ_{min}, is reached, as described in Sec. 2.1.2 in the main paper. Notably, $1 - \sigma_{min}$ represents the share of the base demand for which cutting flexibility is applied.

The summarised parameters for the categories can be found in Table 4 & 5. Fig. 7 depicts the demand profiles and its constituents for all the flexible categories and bidding zone SE3.

Figure 8 illustrates the flexible portion of the total demand, calculated as the yearly average demand subject to shifting flexibility, denoted $\hat{d}^{flex,c}$. This is given by:

$$\hat{d}^{flex,c} = \frac{1}{8760} \sum_{t=0}^{8760} d_t^{flex,c}$$

where $d_t^{flex,c}$ represents the flexible demand for category c at each hour t. It is important to recognize that each demand category exhibits distinct load profiles, as shown in Fig. 7, resulting in varying degrees of available flexibility throughout the year. For example, space heating demand is minimal during the summer months, leading to limited flexibility during this period. Additionally, this calculation does not account for limitations related to τ or the total energy that

can be shifted over time. There appears to be a discernible 1:2:3 relationship among the different sensitivities for total flexibility.
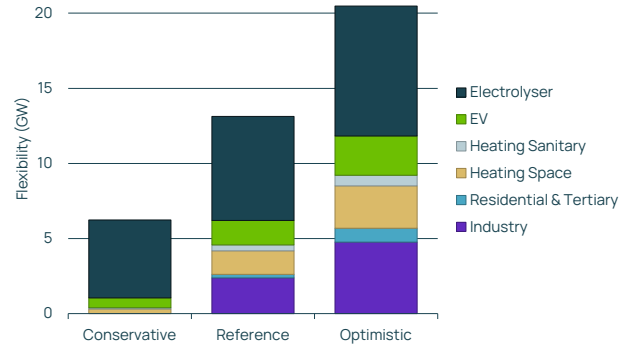

Figure 8: Yearly averaged demand subject to shifting flexibility by category for the different sensitivities aggregated for Sweden in the total demand reference scenario.

2.6. Cost of assumptions of supply technologies

The present investigation establishes a comprehensive framework grounded in a set of overarching financial assumptions essential for our analysis. All monetary values are denominated in real terms, specifically in Euros (€) for the calendar year 2023. This standardization of currency ensures the consistency and precision of our cost assessments. Moreover, our financial considerations encompass the Weighted Average Cost of Capital (WACC), a parameter subject to variation across different sensitivity analyses: reference (6%), optimistic (4%), and conservative (8%). To account for the financial dynamics inherent in project construction phases, we incorporate an interest rate equivalent to half of the WACC during the construction period as a markup on total capital investment. Capital recovery periods are uniformly set at two-thirds of the technical lifetime for all technologies, a measure aimed at preempting the necessity for reinvestment. Details on the calculations of derived costs, such as LCOE and annual investment costs, relevant for the model input, are presented in Sec. 2.6.7.

An integral aspect of our analysis revolves around technology cost assumptions, underpinning both investment and operational considerations. Characteristics for the energy technologies under scrutiny have been determined based on a comprehensive review of references as presented in Tab. 7. These cost estimates are derived from sources spanning pre- and post-transformative landscapes, notably encompassing the significant events of 2022 such as the invasion of Ukraine, the energy crisis, inflationary pressures, and escalating geopolitical tensions. The referenced sources provide insights into historical precedents, contemporary realities, and prospective future projections. Investment and operational costs are examined across three distinct sensitivities: optimistic, base, and conservative, affording a nuanced understanding of potential cost dynamics amidst varying market conditions.

Table 6
Investment and operational cost input assumptions for primary supply technologies. The first and second values within brackets represent optimistic and conservative sensitivities, respectively. The presented LCOE values are purely based on input assumptions. It is worth noting, that the values in brackets here represent combination of all the optimistic and conservative assumptions, respectively.

	Wind Onshore	Wind Offshore	Solar PV	Nuclear
WACC (%)		6 [4, 8]		
Overnight cost (€/kW)	1050 [900, 1200]	2200 [1900, 2700]	500 [375, 625]	5500 [4000, 7000]
Construction time (yr)	1 [1, 2]	1 [1, 2]	0.5 [0.5, 1]	5 [3, 7]
Fixed OM (€/kW-yr)	25 [20, 30]	60 [65, 55]	10	70
Variable OM (€/MWh)	0	0	0	7
Fuel costs (€/MWh)	-	-	-	5
Capacity factor (%)[1]	38	41	11	90 [85, 95]
Economic lifetime (yr)	20	20	23	40
LCOE (€/MWh)[2]	36 [26, 49]	72 [55, 100]	53 [37, 75]	74 [48, 120]

[1]Averaged values, for wind and solar based on weather years 1982-2016, for entire Sweden prior to model results. Includes assumed availability but does not account for economic and grid-related technical curtailment.
[2]Considers only the electricity market, e.g., nuclear revenues from selling heat not considered.

Figure 9 presents a comparison of the overnight capital costs for Solar PV, Wind Onshore and Wind Offshore as well as Nuclear. These figures aim to illustrate the underlying reasoning for the cost assumptions of the present study. To approximate an average cost weighting for investment and operational expenses, representative of the time span from 2024 to 2050 and accounting for technological advancements, we have derived costs based on the year 2040. Compiled investment and operational cost assumptions for for the primary supply technologies are given in Tab. 6 along with the representative LCOE purely based on input assumptions and calculated based on the methodology described in Sec. 2.6.7.

2.6.1. Solar PV

Top-left panel of Fig. 9 illustrates the projected overnight capital costs for utility-scale solar PV as assumed in the present study. The assumptions have been derived from an initial point based on historical average of European countries [20] and learning trends as well as endpoints guided by IEA 2023 [21], with China representing the optimistic scenario, the European Union representing the reference scenario, and the United States representing the conservative scenario. Fixed operational costs have been determined based on TYNDP 2024 [22] to 10 €/kW-yr.

The underlying mechanisms for installing rooftop photovoltaic solar panels have been observed to follow their own trends. Investors are often not large energy producers, but instead companies or private individuals with different views on the profitability of their investment. On this background, rooftop residential solar panel installations have been excluded from the optimisation. Finally, similarly to onshore wind, the Solar PV technology assumes a Greenfield expansion in the model optimisation.

2.6.2. Onshore and offshore wind

In the case of onshore wind, Sweden exhibits relatively low capital costs compared to other European countries, such as Germany, as illustrated in top-right panel of Fig. 9. Generally larger projects, i.e., total power capacity per wind park, for instance due to land constraints, could provide an explanation for the difference (see also Appendix B.5 of Ref. [19]). We have assumed this relationship to continue to hold throughout the modeling horizon. On this background, starting values have therefore been derived from Sweden's historical costs as per IRENA 2023 [20]. Endpoints for optimistic and conservative scenarios are set to approximate the range of cost projections from other references, with a linear learning trend faster in the 2020s compared to the 2030s and 2040s arriving at the assumptions in the current study at 900 (optimistic), 1050 (reference) and 1200 €/kW (conservative). Based on a similar reasoning, fixed operational costs have been set to 20, 25 and 30 €/kW/yr for the optimistic, reference and conservative sensitivities, respectively.

For offshore wind, bottom-fixed foundations represent the sole mature technology. Figure 9, left-bottom panel, compares data from various reference sources, revealing a noticeable scarcity compared to onshore wind. Assumptions for the current study have been set to span the projections at year 2040. Notably, offshore wind installations on floating platforms are anticipated to incur relatively higher costs, as indicated by references such as Ref. [23]. To streamline our analysis, we have opted to standardise all offshore wind cost projections based on bottom-fixed foundations in the current study.

2.6.3. Nuclear

Unlike the typical "learn-by-doing" trends observed in solar PV and wind power, the realm of nuclear power plant construction exhibits significant variations, contingent upon the specific project in question [24, 25]. On this background, a separate methodology has been employed to build the cost sensitivities for nuclear as discussed in detail in the main text. Figure 9, bottom-right panel, illustrates how the

assumptions in the current study compares with other references.

To illustrate, the development of novel nuclear reactor designs in Western Europe has been accompanied by notably high price tags [26], while emerging nuclear power nations such as Türkiye and the United Arab Emirates have realized their initial reactors at relatively lower costs [27, 28]. It is important to recognise that the widespread expectation is that serial construction, i.e., building many reactors of the same kind, and manufacturing of advanced reactor designs, will refine practices, ultimately resulting in cost reductions [29]. Idaho National Laboratory recently published a technical report simulating these potential cost reductions in the US [30] with scenarios largely in congruence with those outlined for the current study.

The projection of the nuclear overnight capital cost employed in the present study is presented in the bottom-right panel of Fig. 9. It is relevant to recognise that the assumed overnight capital cost represents an average cost of several future reactor projects based on a distribution including both successfully and cheaper projects as well as the most extreme outliers on the expensive end. The conservative sensitivity has been constructed such that the average overnight capital cost throughout is 7000 €/kW, reflecting a scenario where future projects experience the similar challenges as the ongoing projects in Europe today with limited learning[5]. On the opposite side, the optimistic sensitivity has been set to average 4000 €/kW mimicking a path with initially more successful projects[6] as well as high learning rate following the successful implementation of dedicated factory serially produced units. The reference sensitivity is placed in between the extremes. Additionally, the construction time for these nuclear units is set to 3 years for the optimistic sensitivity, 5 years for the reference sensitivity, and 7 years for the conservative sensitivity. Operational costs have been set to 70 €/kW-yr [31] for fixed OM and a total cost for variable OM of 12 €/MWh accounting for both cost of fuel (5 €/MWh) as well as spent fuel removal, disposal and long-term storage of spent fuel (7 €/MWh) [32]. As a final note, the current study only considers revenues within the energy-only electricity market. This means that, for instance, nuclear plant potential revenues from selling heat and/or other products are not accounted for.

The existing Swedish nuclear fleet with an assumed total installed capacity of 6.85 GW, *not* including the recent power up-rating[7], is part of the modelling. The power system optimisation allows the retiring of these plants if considered cost effective based on a fixed operational and maintenance cost of 140 €/kW/yr which accounts for necessary reinvestments for life extension [32].

---

[5]Aligning well with Olkiluoto unit 3 at 6900 €/kW (Euronews, 2023, available online).

[6]Aligning well with the average of Barakah units 1-4, WNA (2023), Nuclear Power in the United Arab Emirates. Available online.

[7]https://group.vattenfall.com/se/nyheter-och-press/nyheter/2024/klartecken-for-en-permanent-effekthojning-pa-forsmark-1

2.6.4. Hydro

The existing Swedish hydro power, which was mostly built in the 1950s–80s, is assumed to continue to be in operation in all modelling cases with an assumed installed capacity[8] of 4.56 GW, 6.73 GW, 2.29 GW and 0.24 GW in SE1, SE2, SE3 and SE4, respectively. Modernisation investments in many hundreds of large hydro power plants and dams over a very long period, from the early 2030s to well into the 2060s, will be required. The total system cost for this, described as an annuity that is outside the optimisation analysis, is in the order of €700 million for Sweden [32]. Finally, pumped hydro storage has not been considered.

2.6.5. Bio, natural gas and battery storage

Sweden's combined heat and power fleet is assumed to continue to be in operation with reinvestments such that the current installed production capacity with an average annual generation of around 7 TWh is conserved throughout all modelling cases. The thermal power plants have thus been excluded in the optimisation. Associated reinvestment costs have been neglected.

Limitations on maximum generation of biobased power resources part of the capacity expansion have been defined based on Ref. [32]. Biomass consumption totalling to a maximum corresponding electricity generation of 17.1 TWh applicable to both thermal and combined-heat and power plants. Upper limit of consumption of biogas in open-cycle gas turbine power plants have been set to correspond to an annual generation of 500 GWh.

Table 8 presents the investment and operational costs for further technologies considered in the capacity expansion. For biobased power technologies, biomass-fuelled thermal plants and biogas fuelled open-cycle gas turbines are included. Their investment and cost assumptions have been derived from Ref. [32].

Natural-gas fuelled power plants, including open-cycle and combined-cycle gas turbine (Gas OC & Gas CC) as well as plants equipped with CCS (Gas CCS)[9], employ assumptions derived from Ref. [19] with fuel prices in the reference sensitivity set to 22 €/MWh_th and variations in optimistic to conservative projections from 16 to 28 €/MWh_th. Further fuel price assumptions include biogas with 19.7 €/GJ [22] and biomass with 5.13 €/GJ [12].

Utility-scale battery storage overnight capital costs, for power and energy separately, and operational costs have been derived from ATB 2023 [23]. Notably, both the International Energy Agency (IEA 2023) [21] and ATB 2023 draw upon the same foundational data for battery storage costs, albeit ATB 2023 references a more recent iteration compared to IEA 2023. Additionally, the present study does not separate battery storage technologies by its storage duration. Instead, a generic battery storage technology is considered, subject to

---

[8]Based on highest observed power output in recent years. Theoretical installed capacity is typically higher.

[9]Notably, merely Gas OC is allowed in the capacity expansion for Swedish bidding zones but further technologies are defined for other bidding zones part of the model.
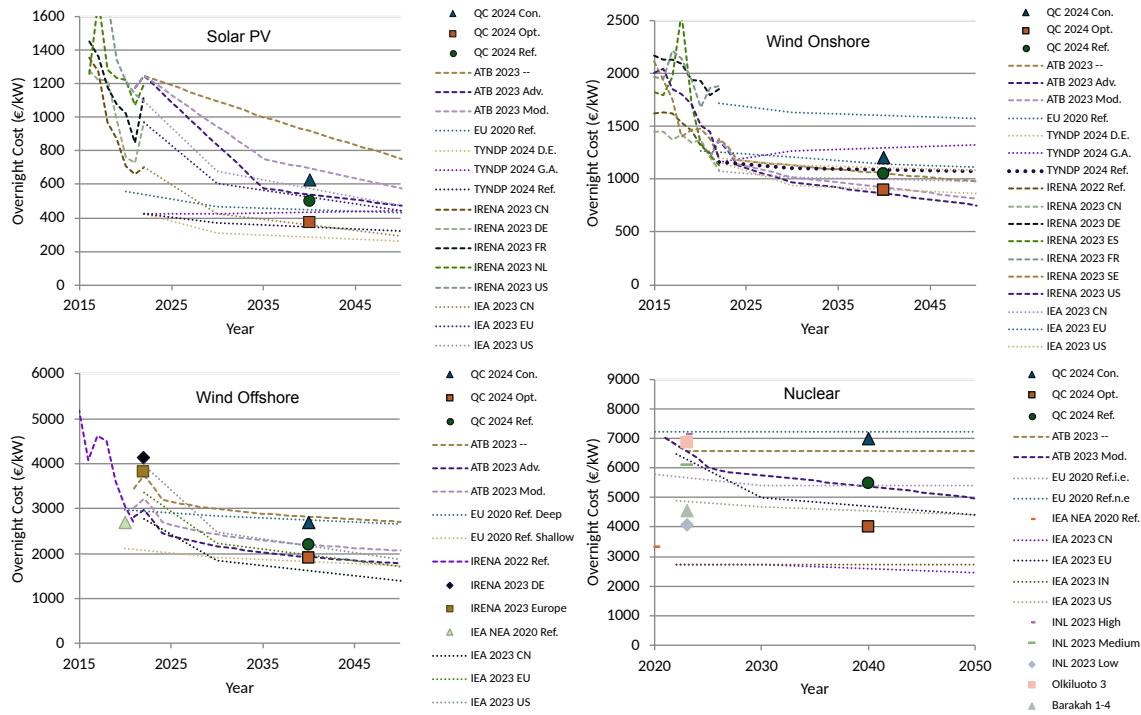
Figure 9: Comparison of overnight capital costs for Solar PV (top-left), Wind Onshore (top-right), Wind Offshore fixed (bottom-left) and Nuclear (bottom-right) in the present study with those from other references, as specified in the legend (see also Tab. 7). The data points are differentiated by markers and line styles: single-point series feature square markers, series with yearly frequent data are represented by dashed lines, and series with multi-year intervals between data points are denoted by dotted lines with circle markers. Assumed values for the current study are placed at year 2040 assumed being representative of the time span 2024 to 2050. Grid connection costs are included for offshore wind.

Table 7

Main source of references building investment and operational cost estimates for power technologies considered.

Reference	Type
National Renewable Energy Laboratory (2023), Annual Technology Baseline.	Future projections, 2021 - 2050
International Energy Agency & Nuclear Energy Agency (2020), Projected Costs of Generating Electricity.	Present-day/near future
International Renewable Energy Agency (2022), Renewable Power Generation Costs in 2021.	Historical
International Renewable Energy Agency (2023), Renewable Power Generation Costs in 2022.	Historical
Energiforsk (2021), El Från Nya Anläggningar.	Present-day/near future
Idaho National Laboratory (2023), Literature Review of Advanced Reactor Cost Estimates.	Present-day/near future
European Commission (2021), EU Reference Scenario 2020.	Future projections, 2020 − 2050
Ten-Year Network Development Plan 2024 (2023).	Future projections, 2022 − 2050
International Energy Agency (2023), World Energy Outlook 2023.	Future projections, 2022 − 2050

the constraint that the storage duration falls within the range of 2 to 10 hours.

2.6.6. Hydrogen - production, storage and power

The model optimisation includes the possibility to build gas turbine power plants fuelled with hydrogen. The gas turbines are fuelled with hydrogen from a zone-by-zone hydrogen storage and the model builds the required electrolyser capacity to produce hydrogen and charge the storage. Cost assumptions for both combined-cycle and open-cycle hydrogen power plants, drawn from an average of ATB 2023 [23] and TYNDP 2024 [22], as well as for lined-rock cavern (LRC) hydrogen storage and electrolysers are presented in Tab. 9.

Table 8
Input cost assumptions for technologies part of the capacity expansion but not presented in the main text. The first and second values within brackets represent optimistic and conservative sensitivities, respectively.

	Biomass [32]	Biogas OC [32]	Gas OC [23]	Battery Storage [23]
WACC (%)	6 [4, 8]	6 [4, 8]	6 [4, 8]	6 [4, 8]
Construction duration (yr)	2	2	2	1
Economic lifetime (yr)	25	17	15	10
Overnight cost (€/kW)	3100	500	640	220 [110, 260]
Overnight cost energy (€/kWh)	-	-		160 [140, 260]
Fixed OM (€/kW/yr)	52	8.4	10	25
Variable OM (€/MWh)	2.2	10	5	0[2]
Fuel (€/MWh)	84 [12]	160 [22]	233[1]	

[1]Includes costs for CO2 emissions for a price 263 €/tCO2.
[2]A cycling cost corresponding to variable costs of 50 €/MWh has been assumed for *existing* battery storage capacity.

Table 9
Input cost assumptions for the production, storage and power from hydrogen. The first and second values within brackets represent optimistic and conservative sensitivities, respectively.

	Hydrogen OC Storage	Hydrogen CC Storage
WACC (%)	6 [4, 8]	
Construction duration (yr)	2	
Economic lifetime power (yr)	20	
Economic lifetime energy (yr)	27	
Economic lifetime charge (yr)	10	
Overnight cost (€/kW)	600	740
Overnight cost energy (€/kWh)[1]	9.7 [1.9, 23]	
Overnight cost charge (€/kW)	680 [530, 840]	
Fixed OM power (€/kW/yr)	10	25
Fixed OM energy (€/kWh/yr)	0	
Fixed OM charge (€/kWh/yr)	29 [16, 41]	
Variable OM power (€/MWh)	5.0	2.5
Variable OM charge (€/MWh)	0[2]	

[1]Annual investment costs weaves in a capacity factor of 0.8.
[2]A cycling cost corresponding to variable costs of 60 €/MWh has been assumed for *existing* electrolyser charging capacity.

The investment costs for electrolysers have been derived from values of IEA 2023 [21] excluding China, with net-zero representing optimistic and stated policies representing conservative sensitivities while the reference sensitivity has been set as the average of optimistic and conservative. The operational costs have been inspired from Ref. [32].

Swedish geological conditions are of hard crystalline rock mass, which is not suitable for underground hydrogen storage solutions such as salt caverns or saline aquifers. However, these geological conditions are ideal for large-scale hydrogen storage in lined rock caverns (LRCs). For this concept, the rock mass provides confinement against the internal gas pressure while the lining keeps the storage completely gas tight. LRCs also allow gas storage at higher internal gas pressures in the order of 200 bar.

The present study assumes no upper limit on hydrogen storage energy capacity. However, an upper limit of 3 weeks for the storage capacity (energy to gas turbine power ratio) was introduced as a constraint for the expansion of the hydrogen storage energy capacity.

To cover a broad spectrum of potential cost scenarios for LRC hydrogen storage [33, 34, 35, 36], the levelised cost of hydrogen storage in the optimistic projection was set to 10 €/kgH2 and 60 €/kgH2 in the conservative sensitivity. The reference sensitivity was set at 30 €/kgH2. Employing a capacity factor of 0.8 and following the calculation methodology described in Ref. [37], we derived the assumptions outlined in Table 9.

2.6.7. LCOE calculations

The Levelized Cost of Electricity (LCOE), denoting the average cost of unit electricity generated by a specific technology, exhibits certain limitations in facilitating meaningful comparisons between technologies. A crucial criterion for capacity expansion is the profitability of all technologies, necessitating their capture price—defined as the average electricity price experienced by the technology—to surpass the LCOE. Transparency of the LCOE constituents ensures a full understanding of input assumptions related to investment and operational costs for various technologies, where the Weighted Average Cost of Capital (WACC) plays a pivotal role.

Nomenclature

a	The annuity factor is used to calculate annualized costs, incorporating the Weighted Average Cost of Capital (WACC) and the project's capital recovery period.
AIC	Annual investment costs (€/MW-yr).
CC	The construction cost represents the upfront cost of building the power generation facility, accounting for construction duration and interest rate.
CF	Capacity factor representing the ratio of the actual electrical energy output over an average weather to the installed power capacity of a technology.
CIR	Construction interest rate, assumed to be half of the Weighted Average Cost of Capital (WACC).

CRP Capital recovery period (yr) or economic lifetime of technology.

ct Construction time (yr).

FC Fuel costs (€/MWh$_{el}$).

FOM Fixed operational and maintenance costs (€/MW-yr).

IC The investment cost (€/MW) is the total investment required for the project, combining the construction cost and the overnight capital cost.

OCC Overnight capital cost (€/MW), which includes eventual grid connection costs.

VOM Variable operational and maintenance costs (€/MWh).

LCOE The Levelized Cost of Electricity (LCOE) is a metric used to determine the average cost of producing one megawatt-hour (MWh) of electricity over the economic lifetime of a power generation project. It combines the initial construction cost, annual fixed and variable operating costs, and the electrical output to provide a standardized measure of the cost of electricity.

MCOE The marginal cost of electricity (€/MWh) represents the additional cost associated with producing one extra MWh of electricity, incorporating variable operating costs and fuel expenses.

WACC Weighted Average Cost of Capital (WACC)

$$CC = OCC \cdot (1 + CIR^{ct}) - OCC \qquad (10)$$

$$IC = OCC + CC \qquad (11)$$

$$a = \frac{\text{WACC} \cdot (1 + \text{WACC})^{CRP}}{(1 + \text{WACC})^{CRP} - 1} \qquad (12)$$

$$AIC = IC \cdot a \qquad (13)$$

$$\text{MCOE} = VOM + FC \qquad (14)$$

$$\text{LCOE} = \frac{AIC + FOM}{8760 \cdot CF} + MCOE \qquad (15)$$

References

[1] The Wind Power, The wind power database, accessed: 2024-09-30 (2023).
URL https://www.thewindpower.net

[2] Länsstyrelserna, LST Vindbrukskollen landbaserade vindkraftverk, accessed: 2024-08-20 (2023).
URL https://ext-geodatakatalog.lansstyrelsen.se/GeodataKatalogen/srv/api/records/GetMetaDataById?id=ed5814b2-08bf-493a-a164-7819e1b590d6

[3] K. Gruber, P. Regner, S. Wehrle, M. Zeyringer, J. Schmidt, Towards global validation of wind power simulations: A multi-country assessment of wind power simulation from MERRA-2 and ERA-5 reanalyses bias-corrected with the global wind atlas, Energy 238 (2022) 121520. doi:10.1016/j.energy.2021.121520.

[4] G. B. Andresen, A. A. Søndergaard, M. Greiner, Validation of danish wind time series from a new global renewable energy atlas for energy system analysis, Energy 93 (2015) 1074–1088. doi:https://doi.org/10.1016/j.energy.2015.09.071.

[5] ENTSO-E, Demand Forecasting Methodology, accessed: 2024-09-30 (2022).
URL https://eepublicdownloads.azureedge.net/clean-documents/sdc-documents/ERAA/2022/data-for-publication/Demand%20Forecasting%20ERAA22.pdf

[6] O. Ruhnau, L. Lundström, L. Dürr, F. Hunecke, Empirical weather dependency of heat pump load: Disentangling the effects of heat demand and efficiency, 19th International Conference on the European Energy Market (EEM) (2023). doi:10.1109/EEM58374.2023.10161914.

[7] et al.. H. Hersbach, ERA5 hourly data on single levels from 1940 to present (2023). doi:10.24381/cds.adbb2d47.

[8] Center for International Earth Science Information Network - CIESIN - Columbia University, Gridded Population of the World, Version 4 (GPWv4): Population Density Adjusted to Match 2015 Revision UN WPP Country Totals, Revision 11 (2018). doi:10.7927/H4F47M65.

[9] International Energy Agency, World Energy Outlook 2022, accessed: 2023-09-21 (2022).
URL https://iea.blob.core.windows.net/assets/830fe099-5530-48f2-a7c1-11f35d510983/WorldEnergyOutlook2022.pdf

[10] Antonini, E. G. A. and Virgüez, E. and Ashfaq, S., et al., Identification of reliable locations for wind power generation through a global analysis of wind droughts, Communications Earth & Environment 5 (2024) 103. doi:10.1038/s43247-024-01260-7.

[11] Qvist Consulting Ltd., Scenario analysis 2050, Tech. rep., Svenskt Näringsliv, accessed: 2024-09-26 (2022).
URL https://www.svensktnaringsliv.se/bilder_och_dokument/rapporter/44s3b3_qcl_snl_290twh_smallfile76pdf_1201114.html/QCL_SNL_290TWh_SmallFile76.pdf

[12] Svenska kraftnät, Långtidsprognos för elanvändningen och anläggningsutbyggnaden 2024–2040, accessed: 2024-02-28 (2024).
URL https://www.svk.se/siteassets/om-oss/rapporter/2024/lma_2024.pdf

[13] Svensk Vindenergi, Statistik, accessed: 2024-09-06 (2023).
URL https://svenskvindenergi.org/statistik

[14] ENTSO-E, Tyndp 2022 regional investment plan - baltic sea, accessed: 2024-07-30 (2022).
URL https://eepublicdownloads.blob.core.windows.net/public-cdn-container/tyndp-documents/TYNDP2022/public/RegIP-2022-BS.pdf

[15] Svenska kraftnät, Årsredovisning 2023, Tech. Rep. 2023/4009, Svenska Kraftnät, accessed: 2024-09-30 (Feb. 2024).
URL https://www.svk.se/siteassets/om-oss/organisation/finansiell-information/svenska-kraftnats-arsredovisning-2023.pdf

[16] Oslo Economics, Gjennomgang av kostnader ved bygging av luftledninger i transmisjonsnettet, Norges vassdrags- og energidirektorat (2019).
URL https://publikasjoner.nve.no/rme_eksternrapport/2019/rme_eksternrapport2019_02.pdf

[17] IEA, Energy technology perspectives 2023, accessed: 2024-09-30 (2023).
URL https://www.iea.org/reports/energy-technology-perspectives-2023/

[18] Swedish Government, Proposal for new energy policy goals (Swedish: Förslag om nya energipolitiska mål), accessed: 2024-07-30 (2023).
URL https://www.regeringen.se/contentassets/01b5f0d6fb8944d0a0ba3f320e7fefdd/forslag-om-nya-energipolitiska-mal-kn202304578.pdf

[19] Quantified Carbon, Power System Expansion Germany: A study by Quantified Carbon for Clean Air Task Force, unpublished (2024).

[20] International Renewable Energy Agency (IRENA), Renewable Power Generation Costs in 2022, accessed: 2024-09-30 (2023).
URL https://www.irena.org/Publications/2023/Aug/Renewable-Power-Generation-Costs-in-2022

[21] IEA, World Energy Outlook 2023, accessed: 2024-09-30 (2023).
URL https://www.iea.org/reports/world-energy-outlook-2023

[22] TYNDP, Ten-Year Network Development Plans (TYNDP) 2024, Tech. rep., ENTSO-E & ENTSOG, accessed: 2024-09-26 (2023).
URL https://2024.entsos-tyndp-scenarios.eu/

[23] National Renewable Energy Laboratory (NREL), Annual technology baseline 2023, accessed: 2024-09-30 (2023).
URL https://atb.nrel.gov/electricity/2023/technologies

[24] J. R. Lovering, A. Yip, T. Nordhaus, Historical construction costs of global nuclear power reactors, Energy Policy 91 (2016) 371–382. doi:https://doi.org/10.1016/j.enpol.2016.01.011.

[25] Energiforsk, Bilagor till rapporten el från nya anläggningar, Tech. rep. (2021).
URL https://energiforsk.se/media/30709/bilagor-till-rapporten-el-fran-nya-anlaggningar.pdf

[26] Institute for Energy Economics and Financial Analysis (IEEFA), European pressurized reactors: Nuclear power's latest costly and delayed disappointments, accessed: 2023-09-27 (2023).
URL https://ieefa.org/articles/european-pressurized-reactors-nuclear-powers-latest-costly-and-delayed-disappointments

[27] World Nuclear Association, Nuclear Power in Turkey, accessed: 2024-09-05 (2023).
URL https://world-nuclear.org/information-library/country-profiles/countries-t-z/turkey.aspx

[28] World Nuclear Association, Nuclear Power in the United Arab Emirates, accessed: 2024-09-05 (2023).
URL https://world-nuclear.org/information-library/country-profiles/countries-t-z/united-arab-emirates.aspx

[29] A. Abou-Jaoude, L. Lin, C. Bolisetti, E. K. Worsham, L. M. Larsen, A. S. Epiney, Literature review of advanced reactor cost estimates (6 2023). doi:10.2172/1986466.

[30] A. Abou-Jaoude, C. S. Lohse, L. M. Larsen, N. Guaita, I. Trivedi, F. C. Joseck, E. Hoffman, N. Stauff, K. Shirvan, A. Stein, Meta-analysis of advanced nuclear reactor cost estimations (6 2024). doi:10.2172/2371533.

[31] NEA, Unlocking Reductions in the Construction Costs of Nuclear, OECD Publishing, Paris, 2020.
URL https://www.oecd-nea.org/jcms/pl_30653/unlocking-reductions-in-the-construction-costs-of-nuclear?details=true

[32] Svenskt Näringsliv, Modellering av svensk elförsörjning - underlagsrapport, accessed: 2024-09-30 (2020).
URL https://www.svensktnaringsliv.se/material/rapporter/modelleringpdf_1144809.html/Modellering.pdf

[33] G. Ripepi, Hydrogen storage for variable renewable electricity integration: Techno-economic analysis of a Lined Rock Cavern system, Chalmers University of Technology, accessed: 2024-09-30 (2018).
URL https://odr.chalmers.se/items/fb0eeba6-3dc6-4ed6-92bb-a2cf40d56b03

[34] H2eart, H2eart for Europe: Report Role of UHS in Europe, accessed: 2024-09-30 (2024).
URL https://h2eart.eu/wp-content/uploads/2024/01/H2eart-for-Europe_Report_Role-of-UHS-in-Europe.pdf

[35] A. S. Lord, P. H. Kobos, D. J. Borns, Geologic storage of hydrogen: Scaling up to meet city transportation demands, International Journal of Hydrogen Energy 39 (28) (2014) 15570–15582. doi:10.1016/j.ijhydene.2014.07.121.

[36] B. Žlender, S. Kravanja, Cost optimization of the underground gas storage, Engineering Structures 33 (9) (2011) 2554–2562. doi:https://doi.org/10.1016/j.engstruct.2011.05.001.

[37] F. Chen, Z. Ma, H. Nasrabadi, B. Chen, M. Z. Saad Mehana, J. Van Wijk, Capacity assessment and cost analysis of geologic storage of hydrogen: A case study in intermountain-west region usa, International Journal of Hydrogen Energy 48 (24) (2023) 9008–9022. doi:https://doi.org/10.1016/j.ijhydene.2022.11.292.